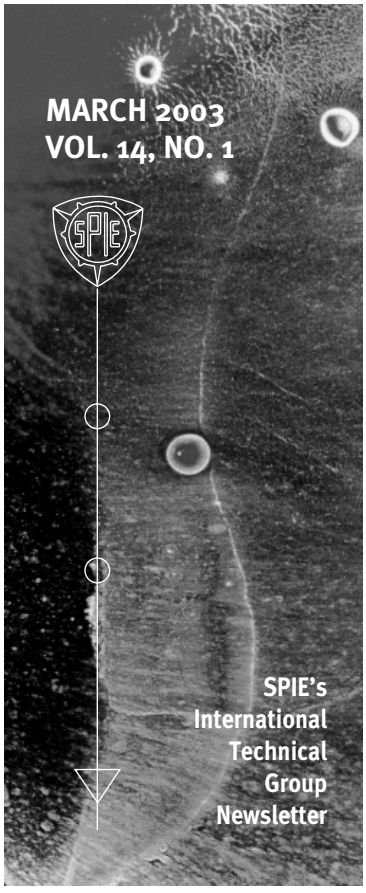


***Calendar***
*—See page 10*

***Technical Group Registration Form*** *—See page 11*

## Newsletter now available online

Technical Group members are being offered the option of receiving the Optics in Information Systems Newsletter electronically. An e-mail is being sent to all group members with advice of the web location for this issue, and asking members to choose between the electronic and printed version for future issues. If you are a member and have not yet received this message, then SPIE does not have your correct e-mail address.

To receive future issues electronically, please send your e-mail address to:
`spie-membership@spie.org`
with the word `OIS` in the subject line of the message and the words `electronic version` in the body of the message.

If you prefer to receive the newsletter in the printed format, but want to send your correct e-mail address for our database, include the words `print version preferred` in the body of your message.


# Optics in Information Systems


## Scalable optical interconnection networks for symmetric multiprocessors (SMPs)

Market demands and application trends, coupled with the ever-increasing need for higher performance and sustained productivity in many scientific applications, are accelerating the need for high-performance, scalable, parallel computing systems. Symmetric multiprocessors (SMPs) are attractive parallel computers and are used widely as they provide a global physical address space and symmetrical access to the entire memory, offering increased flexibility and programmability. SMPs use fast *snoopy* protocols to maintain cache coherence: facilitated by the time-multiplexed, shared bus. Every request is broadcast to all connected modules. As each processor accesses the bus it inserts its address request, which is then *snooped* by all processors and memory modules connected .

Contention problems, combined with the faster processing capabilities of current processors (1-2GHz), degrade the bus's performance. Furthermore, coherence overhead and bus speed (100MHz) limit the number of processors that can be connected, thereby affecting the scalability of snoopy-bus based SMPs. The snoop or address

*Continued on page 7.*

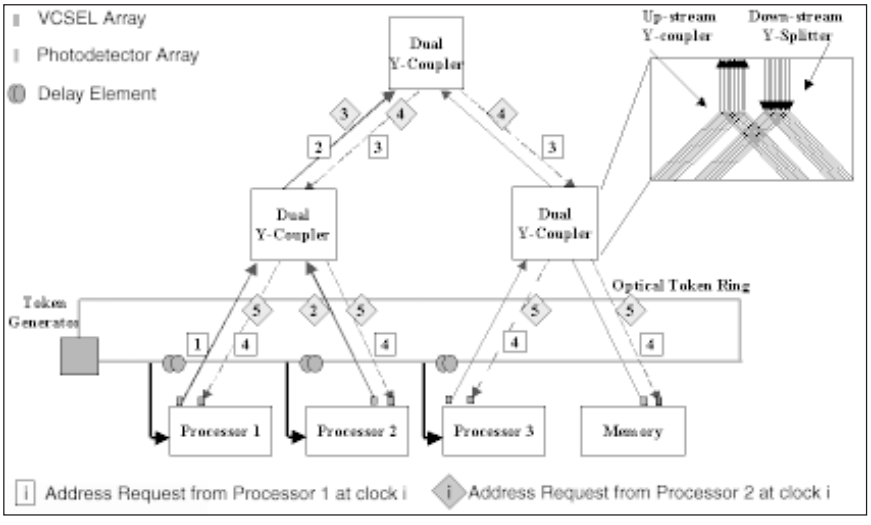


*Figure 1. An overview of a single board of SYMNET, which shows the interconnections for four processors. These are connected to dual Y-couplers by optical waveguides/fibers.*

# Athermal design of WDM holographic filters

Holographic filters can be used for WDM applications, but temperature dependence is a critical concern in telecommunication. Though we can combat thermal drift using thin-film filter technology and clever selection of materials—alternate layers of materials with opposite thermal expansion coefficients can be deposited to fabricate athermal thin-film filters—such flexibility isn't available in bulk holographic filters. In this article we present an athermal design that makes the characteristics of WDM filters (central wavelength, bandwidth, etc.) as invariant as possible with respect to temperature fluctuations.

In our experiments, holographic filters are recorded in lithium niobate ($LiNbO_3$) by interfering two continuous wave laser beams inside the crystal (see Figure 1).[1] A stabilization system has been incorporated into the recording setup in order to prevent the interference pattern from drifting. By properly choosing the angle $2\theta$ between the recording beams, we're able to control the Bragg wavelength of the grating operated in the reflection geometry as a WDM filter (see Figure 2). The reflectance of the filter at normal incidence ($\theta_{out}$=0) is shown in Figure 3 for three different temperatures.

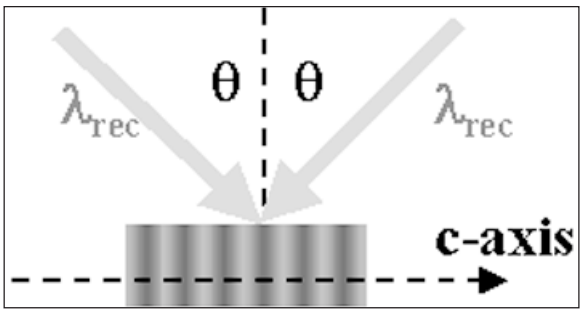


*Figure 1. Recording of a holographic grating.*


*Figure 2. Holographic grating operated as a WDM filter in reflection geometry.*

The Bragg wavelength $\lambda_B$ (center wavelength) of the filter at 24.3°C is estimated to be 1569.45nm with a bandwidth of 0.134nm (~16.75GHz). The criterion used to calculate them is as follows: we first find the two points of the filter whose through-channel transmittances are 0.5dB higher than the minimum transmittance: these are defined as the band edges of the filter. The Bragg wavelength is then calculated as the average of the two edge wavelengths and the bandwidth as the difference between them. We will refer to this as the *0.5dB criterion* from here on.

By inspecting the grating equation:

$$2n\Lambda\cos\theta_{in}=\lambda_B$$

$\Lambda$ is the period of the index grating. We conclude that by tilting the incident beam away from the normal, we're able to Bragg-match the grating to a shorter wavelength.

Temperature changes affect holographic filters mainly through two mechanisms: thermal expansion or contraction of the bulk material (in our case, $LiNbO_3$), i.e. the grating period is a function of temperature; and thermal dependence of the dielectric constant of the bulk material, i.e. the refractive index $n$ is a function of temperature. There are other possible effects—e.g. the thermal dependence of the piezoelectric tensor will manifest itself when stress is being applied—but they will be neglected here.

Within the temperature range of interest, we may assume that both thermal expansion and thermal-dielectric-constant changes are linear. In addition, we know that both coefficients are positive.[2, 3] The athermal design of the WDM filters can therefore be implemented as follows: as temperature rises, the Bragg wavelength of a given filter will shift upward, i.e. towards longer wavelengths. To compensate for such a shift, we tilt the beam away from the normal. On the other hand, to undo the effect caused by a temperature drop, we'll need to adjust the beam towards the normal.

To verify the statement above, we first figure out the *0.5dB criterion* center wavelengths for a series of incident angles at four different temperatures (22.9°C, 41.9°C, 49.1°C, 62.9°C). Temperature monitoring is made possible by reading the resistance off a thermistor in close contact with the $LiNbO_3$ crystal when the whole system is in thermal equilibrium. A thermal-electric cooler is used to control the temperature of the system. The center wavelength corresponding to the incident angle $\theta_{out} = 10°$ ($\theta_{in} \cong 4.5°$) at the lowest temperature is chosen as our target wavelength for angular compensation. For each of the other temperatures, we're able to pick a center wavelength that's closest to the target wavelength along with the corresponding incident angle. We therefore end up with the compensation angle as a function of temperature change. This is plotted in Figure 4.

The fit is done according to the following formula:

$$\frac{\cos(\theta_B + \Delta\theta)}{\cos\theta_B} = \frac{1}{(1+ a\Delta T)(1 + b\Delta T)}$$

Here $a$ is the thermal expansion coefficient, $b$ is the thermal coefficient of dielectric constant, and $\theta_B$ is the Bragg angle corresponding to the target wavelength when $\Delta T = 0$. We conclude

*Continued on page 9.*

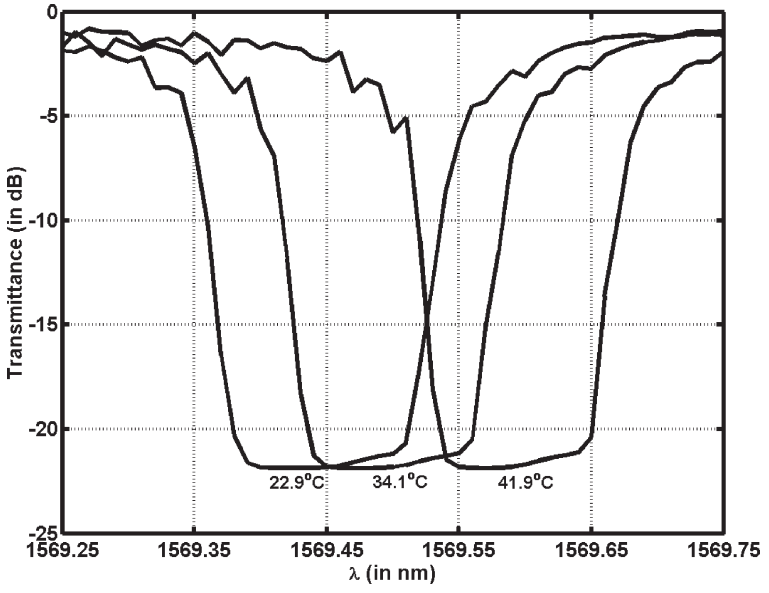


*Figure 3. Filter response measured in the through channel at normal incidence for three different temperatures.*

# Low-power spatial optical interconnection technique for location-based information service environment

In the future, almost all electronic devices will be connected to the broadband information environment. Location-based information services for devices like navigation systems—using GPS (Global Positioning System) or VICS (Vehicle Information and Communication System),[1] for example—will become increasingly important. To realize the appropriate information service environment, a handheld information device—called *My Button*[2]—and a base station—*i-lidar*[3]—have been proposed. My Button has a spatial optical communicating module—called *HV (hyper versatile) target*—to communicate with the i-lidar.

Here we report a novel technique for spatial optical data interconnection using the HV target that uses a liquid crystal light modulator, and we describe an approach to getting a higher data-transfer rate with lower consumption.

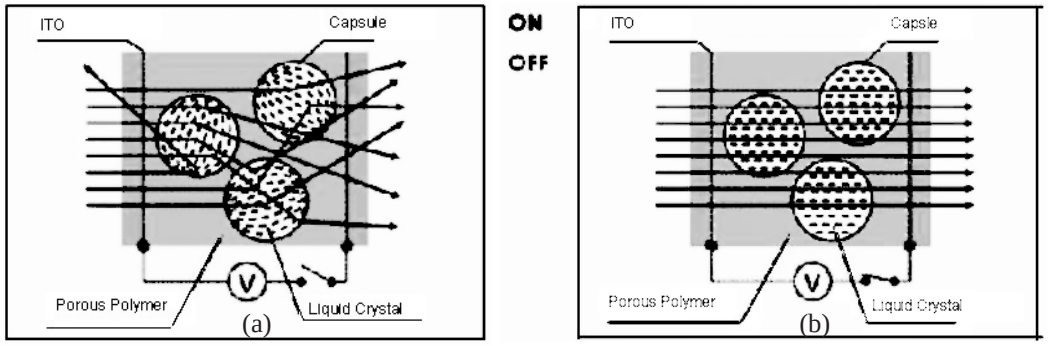


*Figure 1. Operation principle of UMU film: (a) OFF-state (translucent); (b) ON-state (transparent).*

### *Hyper versatile (HV) target*

HV target is a spatial optical communication module that incudes a corner-cube reflector, the reflectivity of which can be varied with low power using a liquid crystal (LC) light modulator. HV target has several implementation levels as shown in Table 1, from simple (level 0) to complicated (level 5).

UMU film[4] is an attractive LC modulator because of its flexibility and polarization insensitivity. Figure 1 shows the principle of UMU film operation. A liquid crystal layer is laminated between two pieces of plastic sheet with a transparent Indium Tin Oxide (ITO) electrode. In the liquid crystal layer, small droplets of nematic LC are dispersed in a porous polymer sheet. When no electric field is applied on the device, the LC molecules are randomly aligned. Consequently, incident light is scattered and cannot pass straight through: it therefore gives the device the appearance of a frosted glass window (translucent). On the other hand, when enough of an electric field is applied to the device, the molecules align in the direction of the field and the light can propagate through the device with relatively little scattering (making it look clear). Thus, transparent optical intensity can be switched with applied voltage without using external polarizing optical devices like conventional LC light modulators.

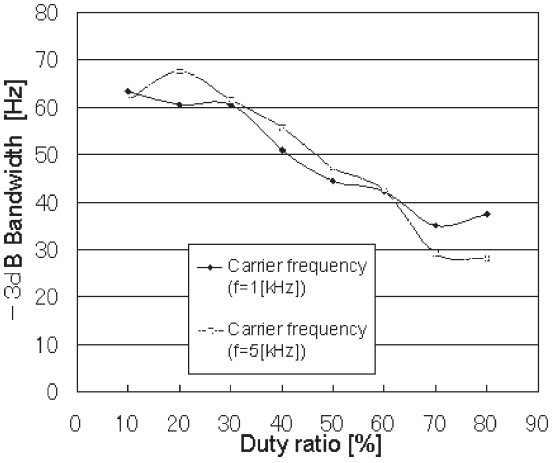


*Figure 2. Modulation frequency characteristics as a function of signal duty ratio.*

**Table 1. Implementation levels of HV targets.**

| | |
|---|---|
| Level 0 | Corner reflector |
| Level 1 | Corner reflector + Liquid crystal light modulator |
| Level 2 | Micro corner reflector array + Liquid crystal light modulator |
| Level 3 | Reflection-type liquid crystal Spatial light modulator |
| Level 4 | reflection-type semiconductor spatial light modulator |

### *Experimental results and discussion*

The response time for the LC to switch from translucent to clear (rise time) at AC24V is 0.4ms. To go from and clear to translucent (fall time) takes 20ms. Figure 2 shows modulation bandwidth characteristics as a function of on/off duty ratio at 1kHz and 5kHz carrier frequencies. Because the fall time is much longer than the rise time, wider bandwidth was measured at the small duty ratio condition. Figure 3 shows eye diagrams with 50%, 25%, and 12.5% duty ratio, at 30Hz, 100Hz, and 300Hz modulation frequency. No eye was observed with 50% duty ratio at 300Hz.

Because the rise time of the UMU film is much faster than fall time, a reduction of the duty ratio is effective for higher modulating speeds. At the maximum, over 100 bps transmission was obtained with a 12.5% duty ratio.

On the other hand, because the download data rate is easily over 100Mbps, the data transfer ratio of download to upload can be more than $10^6$. We call this spatial optical interconnection Asynchronous speed Spatial Optical Broadband Interconnection, *ASOBI*. Despite its large asynchronous data rate, the system can perform useful tasks. For instance, many applications require broadband data download—

*Continued on page 9.*

# Optical interconnection system based on fiber image guides

Optoelectronic interconnection systems can provide high-speed, high-bandwidth data transfer with low power and low crosstalk.[1] In these systems the optical interconnection between transmitter and receiver arrays must be done with low cost, low loss, and tolerance to misalignment. Recently, fiber image guides (FIGs) have been used to transfer two-dimensional (2D) optical data packets as an alternative to free-space interconnections.[2,3] Free-space optical interconnects are very useful for short-distance 2D parallel interconnects but they are not suitable for multi-channel interconnects over long distances (over 1m) because of beam spreading and the difficulty of alignment. FIGs are tightly-packed arrays of thousands of optical fibers, and are capable of 2D parallel image transmission with more flexible alignment and packaging than free-space alternatives.

Figure 1 shows the construction of a typical FIG. Those we used in the experiment are produced at Schott Optovance, Inc. Their density is approximately $10^4$mm$^{-2}$, and each component strand is a step-index multi-mode fiber. The FIGs consist of more than 15,000 of these core fibers, each with a 9.1μm core diameter and 13.6μm pitch. Available numerical apertures (NA) are 1.0, 0.55, and 0.25, and the attenuation level is less than 0.4dBm$^{-1}$ in the wavelength range from 700nm ~ 1100nm. The optical attenuation of 0.25 FIGs is even lower at 0.1dB/m. The individual fibers are rigidly bounded to each end by a background acid-soluble glass holder 2.5cm thick. Between these points the individual fibers are loose so that the FIG can be bent and positioned easily.

We interconnect two or more transceiver arrays by mounting each FIG end close to a transmitter and detector array. Great freedom in alignment and packaging is possible thanks to the FIG flexibility: optical alignment is easily achieved by moving the bundle ends. We mounted the image guides between two optoelectronic transceiver array boards called Transpar:[4] a modular optoelectronic interconnection test system containing a field-programmable gate array (FPGA) chip for reconfigurable logic, vertical-cavity surface-emitting laser/metal-semiconductor-metal (VCSEL/MSM) smart-pixel devices for optical input/output, and transimpedance receiver arrays.

Transpar can implement both a photonic multi-token ring network and signal processing functions on three-dimensional data packets being transferred among nodes. The distance between each VCSEL/detector and FIG is critical in determining optical power and beam collimation. There are three different distance variables in our setup. The distance between the top of the VCSELs and the input end of the FIG is given by $d_{in}$, the distance between the output end and the detector plane is $d_{out}$ and the distance along the length of the FIG from the input end is given by $d_{FIG}$.

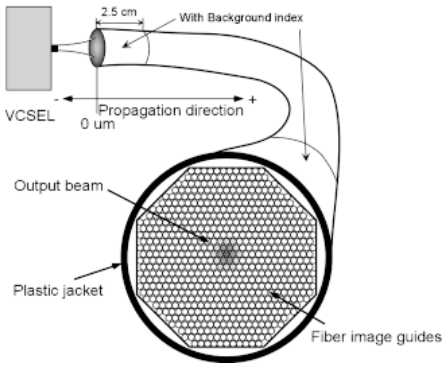


*Figure 1. Fiber image guide structure.*

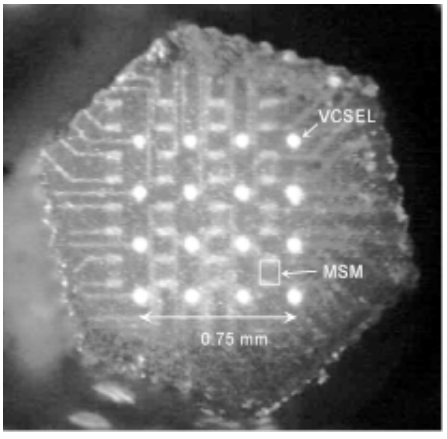


*Figure 2. FIG output image of Honeywell VCSEL-MSM chip.*

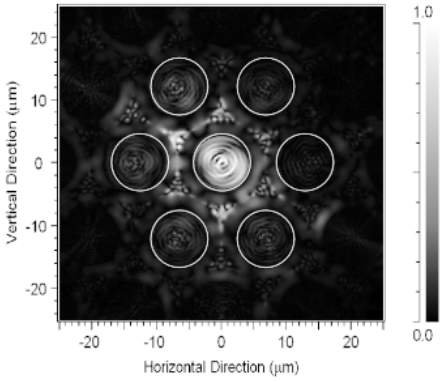


*Figure 3. Transverse field profile outputs of a VCSEL through fiber image guides.*

To optimize the interconnection efficiency, it is important to match the optical spot size to the detector size. The MSM detector size is about 75×75μm, so we need the optical spot size to be less than 75μm in diameter. We observed the spot using a CCD camera directly from the image guide output as shown in Figure 2. The output spot size is well defined and less than 75μm in diameter when the coupling distance $d_{in}$ is less than 100μm.

A detailed computer simulation of waveguide propagation in a FIG was investigated using RSoft's BeamPROP. The simulations were performed on different *x-y-z* directional alignments to analyze the optical power output. The maximum power output is obtained when the center of the laser aperture is well aligned to the core fiber. Figure 3 shows one simulation result with $d_{in}$ = 100μm, $d_{FIG}$ = 200μm, $d_{out}$ = 0μm. The core fiber boundaries are shown by white circles. For the simulation we launched a 15μm-wide laser in various launch positions. These simulations are well supported by the experimental results.

**Sunkwang Hong and Alexander A. Sawchuk**
Signal and Image Processing Institute
Integrated Media Systems Center
University of Southern California, Los Angeles, CA 90089-2564
Tel: +1 213/740-4622
Fax: +1 213/740-4651
E-mail: sawchuk@sipi.usc.edu

**References**

1. Special Issue on Optical Interconnections for Digital Systems, **Proc. IEEE 88** (6), June 2000.
2. D. M. Chiarulli, S. P. Levitan, P. Derr, R. Hofmann, B. Greiner, and M. Robinson, *Demonstration of a Multichannel Optical Interconnection by Use of Imaging Fiber Bundles Butt Coupled to a Optoelectronic Circuits*, **Appl. Opt**. **39,** pp. 698-703, 2000.
3. S. Hong and A. A. Sawchuk, *Testing and Simulation of an Optical Interconnection System Using Fiber Image Guides*, **Proc. SPIE 4987, 2003**
4. S. Hong, Z. Y. Alpaslan, L. Zhang, C. Min, and A. A. Sawchuk, *Testing of Reconfigurable Translucent Smart Pixel Array (R-Transpar) for Optical Multi-Token-Ring Network*, **International Topical Meeting on Optical Computing, (OC 2002)**, pp. 141-143, Taipei, Taiwan, April 2002.

# Holding light assists four-wave-mixing-based semiconductor wavelength converters

All-optical wavelength conversion using the four-wave mixing (FWM) effect in a semiconductor optical amplifier (SOA) can provide functions necessary for optical networks. However, the technique suffers from poor conversion efficiency. Significant improvement both here and in the noise figure are required to make the technology practical for application. FWM conversion efficiency increases approximately with the square of the unsaturated gain and saturation intensity.[1] Consequently, increasing the gain and/or saturation power of a SOA is the key to improve conversion efficiency. A holding light, also called an assisting beam, was suggested as a way of increasing the saturation intensity of the SOA.[2,3] We will demonstrate that using such a beam can also improve the efficiency and signal-to-noise ratio of a FWM-based wavelength converter.

The effect of an assisting beam on wavelength conversion depends on what happens as the beam passes through the SOA. When the device is operated in the gain regime for the assisting light, the saturation intensity is raised but the amplifier gain lowered. If the SOA is biased in the absorptive regime, both its gain and saturation power can be increased. However the current required for this condition is usually too small to provide enough gain for wavelength conversion. Finally, if the SOA is operated at or close to the transparent condition for the assisting beam, the saturation intensity can be enhanced without sacrificing the gain.

Figure 1 shows the schematic of a light-assisted wavelength converter. A high-power assisting beam is propagates through the SOA in the opposite direction as the pump and probe beams. The latter two beams interact inside the SOA to generate a conjugated signal through nonlinear effects. To prove the improvement in wavelength-conversion efficiency with an assisting beam, the measurement was carried out using two different wavelengths: 1480nm or 1430nm. The output signal was measured with an optical spectrum analyzer (OSA) that can clearly distinguish the conjugated signal from the amplified spontaneous emission noise (ASE). The conversion efficiency can be enhanced by 5.8dB at the corresponding transparent current for the 1480nm assisting beam when the detuning (frequency spacing between the pump and probe wavelengths) is 100Gbps. The enhancement increases slightly as the detuning becomes larger. The enhancement drops to 3.3dB when the SOA bias is raised to 200mA. This is due to the fact that the assisting beam increases the saturation power but decreases the available gain.

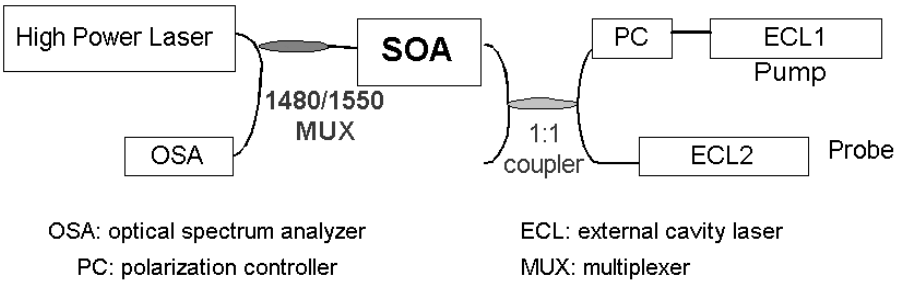


*Figure 1. Schematic of wavelength conversion using the FWM effect of a SOA and an assisting beam.*

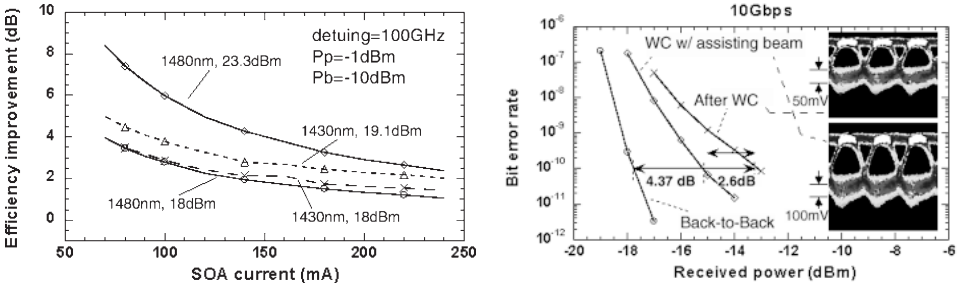


*Figure 2. Performance enhancement of wavelength conversion by using an assisting beam: (a) improvement of conversion efficiency at different bias currents for 1480nm and 1430nm assisting beams; (b) bit error rate and eye diagrams.*

In principle, it is possible to use a shorter-wavelength assisting beam—one whose transparent current is higher—to obtain larger enhancement at high SOA bias. Figure 2a shows that the assisting beam provides for larger improvement at 1430nm than 1480nm for the same assisting power (18dBm). In fact, the difference between the results of using 1480nm or 1430nm is not as significant as expected due to the fact that the gain for the assisting beam depends on its wavelength. With a 200mA bias, which is closer to the transparent current for the 1430nm beam, the net gain is larger for the 1480nm assisting beam. Therefore, the larger enhancement to wavelength conversion efficiency by using a shorter-wavelength assisting beam is compensated by the smaller net gain. The advantage gained by using a shorter-wavelength assisting beam is more pronounced at higher SOA bias currents, where the 1480nm beam depletes more carriers than the 1430nm beam does. Also, the gain difference provided by the SOA to the assisting beam of different wavelengths tends to be smaller at higher bias.

In addition to the improvement to conversion efficiency, the assisting beam can increase the signal-to-background-noise ratio (SBR) by about 3dB and 1.5dB at the bias levels of 105mA and 200mA, respectively. The measured FWM spectra indicate that the presence of an assisting beam also increases ASE, but it is less than the increase in the conjugated signal. The improvement on the conversion efficiency and SBR by using an assisting beam can be seen clearly by measuring the eye-diagram for the received signals when the probe beam is modulated at 10Gbps data rate. The results are shown in the inset to Figure 2b. The 1480nm assisting beam increases the signal amplitude by >5dB at 105mA and by >1.5dB at 200mA. Without using an assisting beam, the conjugated signal after wavelength conversion suffers from a 4.4dB power penalty due to the contribution from the signal-spontaneous-emission noise, as shown in Figure 2b. The power penalty is reduced by 2.6dB when an assisting beam is applied. This proves that the assisting beam improves not only the conversion efficiency but also the signal quality of a FWM-

*Continues on page 9.*

# Integrated optical devices based on a lithium niobate substrate

We have developed integrated optical devices based on lithium niobate ($LiNbO_3$). Integrated optical bistable circuits consisting of two parallel reversed-$\Delta$-directional couplers interconnected by single mode waveguides were fabricated on a single $LiNbO_3$ crystal, as shown in Figure 1.[1] Hybrid optical bistable performance was demonstrated. By controlling parameters of the applied dc voltage, both the complementary and consistent types of hysteresis loops and differential curves are obtained. Optical logic gates and optical amplifiers can therefore be constructed.

In information and optical communication systems, external modulation of laser sources has been employed for high speed applications. The Mach-Zehnder modulator based on $LiNbO_3$ has been widely used for this purpose. However, the linearity of the output optical signal is a critical issue because of the induced Bessel-function distortions of the Mach-Zehnder modulator. The cascaded modulator structure was therefore investigated to reduce the harmonic and intermodulation distortions.[2] Distortions of -47dB and -39dB can be obtained, respectively, using this structure.

To evaluate the performance of integrated optical devices used in information and optical communication systems, the propagation loss for an optical channel waveguide is a very important issue. We developed a nondestructive method for measuring the propagation and bending losses of separated individual modes within single- and multimode waveguides. This novel technique is a combination of the butt-couple, prism-couple, and phase-modulation methods.[3,4]

To reduce the bending propagation loss for integrated optical devices, the microprism structure was investigated. To construct a low-loss and wide-branching-angle symmetric Y-junction waveguide, a novel structure with full phase compensation was used.[5,6] The structure, as shown in Figure 2, consists of a pair of microprisms for pre-compensation and a microprism for phase-front acceleration. A normalized transmitted power of more than 95% is obtained, even though the branching angle of the Y-junction waveguide is up to 20°.

**Ching-Ting Lee**
Institute of Optical Sciences
National Central University
Chung-Li, Taiwan
Republic of China

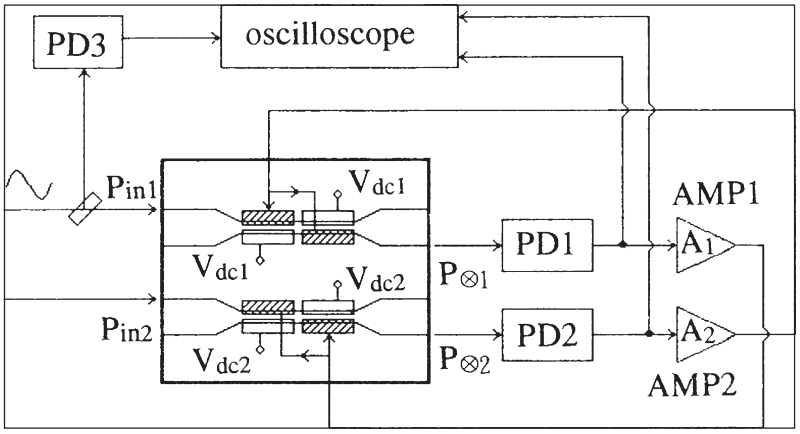


*Figure 1. Experimental setup of the complementary optical bistable operator.*

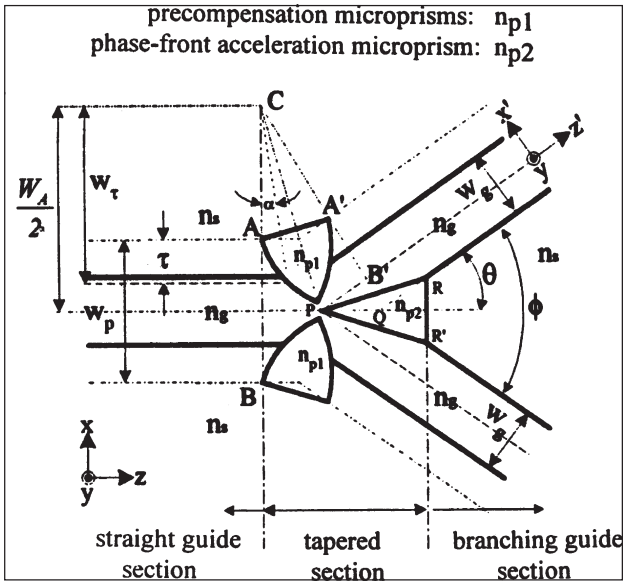


*Figure 2. Top view of the full-phase-compensation microprism-type Y-junction waveguide.*

**References**

1. C.T. Lee, H.C. Lee, H.H. Lai, and L.G. Sheu, *Complementary optical bistable operation with integration of two directional couplers on $LiNbO_3$ crystal*, **Jpn. J. Appl. Phys. 35** (5A), p. 2686, May 1996.
2. C.T. Lee, H.C. Lee, and L.G. Sheu, *The reduction of harmonic and intermodulation distortions with a cascaded Mach-Zehnder modulator,* **Opt. Rev. 3** (5), p. 341, 1996.
3. C.T. Lee, *Nondestructive measurement of separated propagation loss for multimode waveguides,* **Appl. Phys. Lett. 73** (2), p. 133, July, 1998.
4. C.T. Lee, *Nondestructive measurement of individual modes loss for waveguides,* **U.S. Patent US6219475B1**.
5. J.M. Hsu and C.T. Lee, *Design of microprism-type symmetric Y-junction waveguides with the full phase compensation method,* **Appl. Opt. 38** (15), p. 3234, May 1999.
6. J.M. Hsu and C.T. Lee, *Systematic design of novel wide-angle low-loss symmetric Y-junction waveguides,* **IEEE J. Quantum Electron. 34** (4), p. 673, April 1998.

# Scalable optical interconnection networks for symmetric multiprocessors (SMPs)

*Continued from cover.*

bandwidth required to broadcast the address requests is, therefore, the major limitation of SMPs. Electrical solutions to this address bandwidth have ranged from using split-transaction or multiple-address buses, or a data crossbar (such as UE10000[1] from Sun) that can scale up to 64 processors. Beyond this, the address buses are saturated.

Optical technology can provide the high communications bandwidth needed to solve the address bandwidth limitation. The key technology is the low-cost, parallel, optical interconnects consisting of an array of vertical-cavity surface-emitting lasers (VCSELs) and photodetector (PD) transceivers with data rates in excess of 3Gb/s per channel.[2] An array of such transceivers enable address transmission at a rate of 200-300Gbps, which will be the address bandwidth required by future SMPs. The proposed optical symmetric multiprocessor, called SYMNET, consists of four processors interconnected using a binary tree is shown in Figure 1. The tree is constructed using a dual array of Y-couplers that allow two-way address transmission (see inset to Figure 1). The up-stream array of Y-couplers is used to combine the address requests from the processors. After reaching higher levels, these address requests are rerouted through the downstream array of Y-splitters, enabling the broadcast of the address requests to all the processors and memories.

Time-division multiple-access (TDMA) protocol is used as a control mechanism to achieve mutually-exclusive access to the shared channel. Optical token propagation ensures that address requests are transmitted from successive processors without collision. This way, address requests from different processors can be pipelined and more than one address request can be inserted into the tree interconnect.[3] The optical token is a single pulse that provides a time reference for insertion of address requests into the tree interconnect by the individual processor. As shown in Figure 1, in cycle 1 (square) the optical token is received by processor 1, which in turn transmits an address request. In cycle 2, when this address from processor 1 is in propagation at the next level of the tree, the token is received by processor 2, which can transmit its own address request (shaded diamonds). In cycle 3, the address request from processor 1 is being re-routed using the downward Y-splitter, and at the same time the address request from processor 2 has moved up the binary tree. The optical token is now received by processor 3, which can transmit an address. In cycle 4, the address request from processor 1 has reached all the processors, and all snoop for it simultaneously. Broadcasting the address request results in simultaneous reception and snooping of the request by all the processors/memory modules. The address requests are thereby serialized.

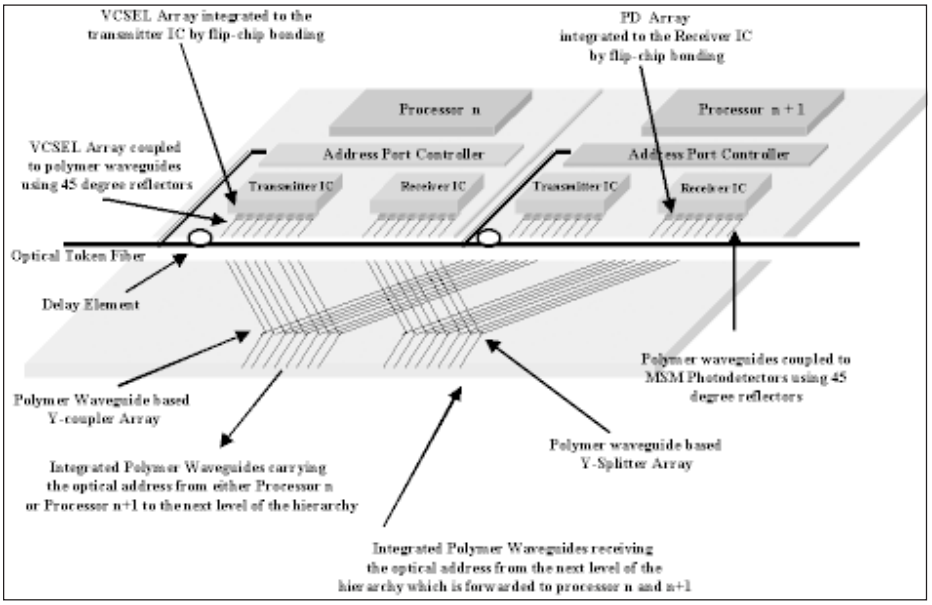


*Figure 2. The proposed optical implementation of SYMNET using parallel optical interconnects, polymer waveguides, SOAs, and an array of Y-couplers/splitters, is shown.*

A possible optical implementation of SYMNET using parallel optical transceivers, polymer waveguides, arrays of Y-couplers/splitters, and semiconductor optical amplifiers, is shown in Figure 2. Parallel optical links—1D and 2D (1×12, 4×12, and 6×12) VCSEL arrays operating in the 850-980nm wavelength range at 3Gbps/channel data rate—are commercially available. There are several methods for integrating VCSELs with optical receivers such as standard complementary metal-oxide silicon (CMOS) circuitry. These include substrate removal, coplanar flip-chip bonding (for bottom-emitting VCSELs), and various top-contact bonding methods.[4] We use polymer waveguides to route the optical address requests from the discrete processors as they exhibit excellent thermal stability, low optical loss and mechanical robustness.[5] Y-couplers/splitters are efficient at splitting light, but the associated losses are tremendous for a given BER. Hence, we use an array of semiconductor optical amplifiers (SOAs) at the root of the tree to boost the power of the optical address request. SOAs operating in the 980nm range provide a fiber-to-fiber gain of 20dB with a response time of less than 60psec.[6] The address request is fed to the CMOS transmitter IC through the address-port controller, which in turn drives the VCSELs. The direction of the light launched into the waveguides is changed by 90° using a 45° reflector. The address pulses propagate in the waveguides through different levels of couplers and splitters. At the receiving end of the waveguides, the direction of light pulses is once again changed by 90°. The light pulses are eventually received by the photodetector after amplification, and are returned to the address-port controller from the CMOS receiver IC for processing the received address request.

Figure 3 shows the layout of the tree-based address sub-network interconnecting the various processors through different levels of the system boards. At the intra-board level (k=0), 2-4 processor/memory modules are connected using polymer-waveguide-based arrays of up-stream Y-couplers and down-stream Y-splitters. At the next level (k=1), similar couplers and splitters are connected from different intra-boards. At the highest level (k=2), these up-stream and down-stream couplers are connected to an array of SOAs. The optical pulses are routed using waveguides at the intra-board/inter-board levels, and between boards using polymer fibers. MT-ferrule-type push-pulls are used to connect the waveguides and fibers.[7] The system can be scaled in powers of two by simply replicating it and then adding to it. The addition of newer boards is facilitated by disconnecting the root board (level k=n), inserting another board between it and level k=n-1, and then re-connecting the root board to the new one. Hence, SYMNET provides easy addition of boards without significantly altering the ex-

*Continues on page 8.*

## Scalable optical interconnection networks for symmetric multiprocessors (SMPs)

*Continued from page 7.*

isting architecture. This facilitates the scalability of the address sub-network.

Cache coherence cannot be maintained by using standard snoopy protocols: they must be modified to take into account the simultaneous insertion of address requests into the tree interconnect. By adding transient states to the existing stable states, it is possible to satisfy cache coherence and sequential memory consistency requirements. The theoretical power-budget analysis reveals a high scalability: as many as 128 processors could be supported by this architecture for a BER of $10^{-15}$ at an operating wavelength of 980nm.

**Ahmed Louri and Avinash Karanth Kodi**
Department of Electrical and Computer Engineering
University of Arizona
Tucson, AZ 85721
E-mail: louri@ece.arizona.edu

**References**

1. A. Charlesworth, *STARFIRE: Extending the SMP Envelope*, **IEEE Micro 18** (1), pp. 39-49,1998.
2. *Parallel Links transform network equipment*, **FiberSystems International**, pp. 29-32, Feb 2002.
3. Donald M. Chiarulli, Stephen P. Levitan, Rami G. Melhem, Manoj Bidnurkar, Robert Ditmore, Gregory Gravenstreter, Zicheng Guo, Chungming Qiao, Majd F. Sakr, and James P. Teza, *Optoelectronic Buses for High-Performance Computing*, in **Proc. IEEE 82** (11), pp. 1701-1710, 1994.
4. R. Pu, E. M. Hayes, C. W. Wilmsen, K. D. Choquette, H. Q. Hou, and K. M. Geib, *Comparison of techniques for bonding VCSELs directly to ICs*, **J. Opt. A: Pure and App. Opt. 1** (2), pp. 324-329, 1999.
5. Louay Eldada and Lawrence W. Shacklette, *Advances in Polymer Integrated Optics*, **IEEE J. Selected Topics in Quantum Electronics 6** (1), pp. 54-68, Jan/Feb 2000.
6. D. Wiedenmann, C. Jung, M. Grabherr, R. Jager, U. Martin, R. Michalizk, and K. J. Ebeling, *Oxide-confined vertical-cavity semiconductor optical amplifier for 980nm wavelength*, **Technical Digest Lasers and Electro-Optics**, pp. 378-379, 1998.
7. Y. S. Liu, R. J. Wojnarowski, W. A. Hennessy, J. P. Bristow, Yue Liu, A. Peczalski, J. Rowlette, A. Plotts, J. Stack, M. Kader-Kallen, J. Yardley, L. Eldada, R. M. Osgood, R. Scarmozzino, S. H. Lee, V. Ozgus, and S. Patra, *Polymer Optical Interconnect Technology (POINT)-Optoelectronic Packaging and Interconnect for Board and Backplane Applications*, **Proc. Electronic Components and Tech. Conf.,** pp.308-315, 1996.

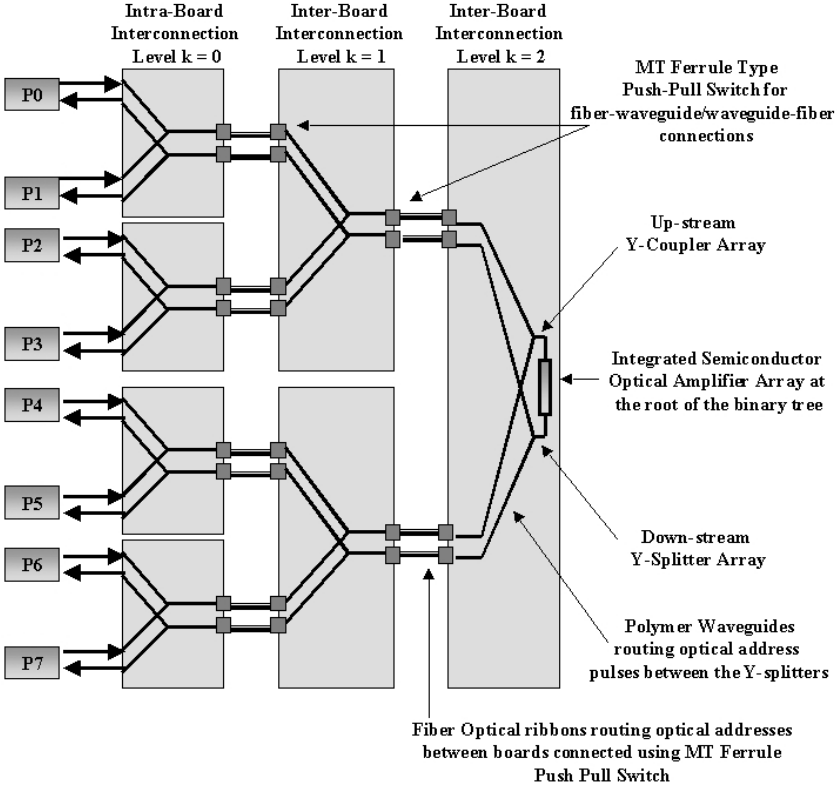


*Figure 3. Shown is a complete layout illustrating the interconnections between discrete processors/memories using polymer waveguides, with fiber ribbons at the intra-/inter-board levels.*

## Planar integration of complex systems for optical communication and computing

*Continued from page 12.*

routed onto a 2D optoelectronic chip in the center that is set up as a smart pixel array. It contains detectors, via which the switch matrix can be programmed optically, and modulators for the actual switching. The linear detector array that acts as the final stage of the crossbar switch has not yet been bonded to the substrate in the setup of Figure 2. It could be shown that optical signals can be reliably routed onto their respective targets with this demonstrator.

For bridging larger interconnection distances, optical fiber links can be attached to planar-integrated MOEMS. Experimentally, an approach using fiber ribbons with standard MT-type connectors that are attached via a micromachined socket plate was realized.[5] This allows one to connect cables with 12 optical fibers. Here, reliable fiber-free-space optical links could also be established. Future research now has to tackle the problem of improving the coupling efficiency: it's been ignored so far in the above proof-of-principle experiments.

**Matthias Gruber and Jürgen Jahns**
FernUniversität Hagen
Universitätsstr. 27
58084 Hagen, Germany
Tel: +49 2331 987 1131
Fax: +49 2331 987 352
E-mail: Matthias.Gruber@FernUni-Hagen.de

**References**

1. J. Jahns and A. Huang, *Planar integration of free-space optical components*, **Appl. Opt. 28,** p. 602, 1989.
2. S. Sinzinger and J. Jahns, *Integrated micro-optical imaging system with a high interconnection capacity fabricated in planar optics*, **Appl. Opt. 36,** p. 4729, 1997.
3. D. Fey, W. Erhardt, M. Gruber, J. Jahns, H. Bartelt, G. Grimm, L. Hoppe, and S. Sinzinger, *Optical Interconnects for Neural and Reconfigurable VLSI Architecture*, **Proc. IEEE 88,** p. 838, 2000.
4. W. Eckert, S. Sinzinger, and J.Jahns, *Compact planar-integrated optical correlator for spatially incoherent signal*, **Appl. Opt. 39**, p. 759, 2000.
5. M. Gruber, J. Jahns, E. El Joudi, and S. Sinzinger, *Practical Realization of Massively Parallel Fiber-Free-Space Optical Interconnects*, **Appl. Opt. 40,** p. 2902, 2001.

## Athermal design of WDM holographic filters

*Continued from page 2.*

that, by slightly tilting the incident beam, we're able to compensate for Bragg wavelength drifts due to changes in the ambient temperature.

Our data suggest that, for operation around an incident angle $\theta_{out}$ of 10°, an angular correction of 0.88° will be required for a temperature change of 100°C. Such an angular fine-tuning can be achieved by a bimetallic composite beam, which makes use of the TEC (thermal expansion coefficient) discrepancy between two properly chosen materials.[4] The principle of operation is illustrated in Figure 5. The aluminum-silicon composite beam will be designed in such a way that it deflects 0.44° for a temperature change of 100°C.

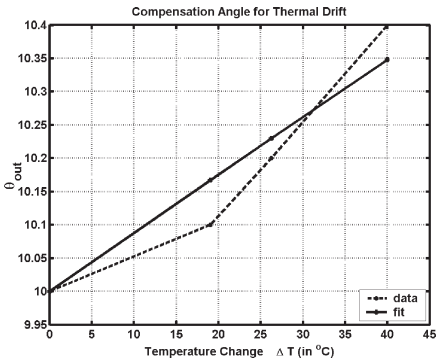


*Figure 4. Compensation angle for thermal drift of Bragg wavelength as a function of temperature change.*

**Hung-Te Hsieh, George Panotopoulos, and Demetri Psaltis**
California Institute of Technology
MS 136-93
Pasadena, CA 91125
E-mail: TeTe@sunoptics.caltech.edu

**References**

1. G. A. Rakuljic and V. Leyva, *Volume holographic narrow-band optical filter,* **Optics Letters 18** (6), p. 459, 15 March 1993.
2. R. T. Smith and F. S. Welsh, *Temperature dependence of elastic, piezoelectric, and dielectric constants of lithium tantalite and lithium niobate,* **Journal of Applied Optics 42** (6), p. 2219, May 1971.
3. U. Schlarb and K. Betzler, *Refractive indices of lithium niobate as a function of temperature, wavelength, and composition – a generalized fit,* **Physical Review B 48** (21), p. 15613, 1 December 1993.
4. W. H. Chu, M. Mehregany, and R. L. Mullen, *Analysis of tip deflection and force of a bimetallic cantilever microactuator,* **Journal of Micromechanics and Microengineering 3**, p. 4, 5 February 1993.

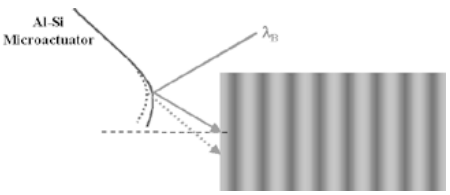


*Figure 5. Athermal design utilizing an Al-Si composite beam microactuator.*

## Holding light assists four-wave-mixing-based semiconductor wavelength converters

*Continued from page 5.*

based wavelength converter.

**San-Liang Lee**
Professor, Dept. of Electronic Engineering
Director, Center for Optoelectronic Science and Technology
National Taiwan University of Science and Technology
Tel: +11 886 2737 6401
Fax: +11 886 2737 6424
E-mail: sanlee@et.ntust.edu.tw

**References**

1. A. D'Ottavi, F. Martelli, P. Spano, A. Mecozzi, and S. Scotti, *Very high efficiency four-wave mixing in a single semiconductor traveling-wave amplifier*. **Appl. Phy. Lett. 67,** pp. 2753-2755, 1995.
2. M. A. Dupertuis, J. L. Pleumeekers, T. P. Hessler, P. E. Selbmann, B. Deveaud, B. Dagens, and J. Y. Emery, *Extremely fast high-gain and low-current SOA by optical speed-up at transparency*, **IEEE Photon. Technol. Lett.**, 12 (11), pp. 1453-1455, Nov 2000.
3. M. Yoshino and K. Inoue, *Improvement of saturation output power in a semiconductor laser amplifier through pumping light injection*, **IEEE Photon. Technol. Lett. 8** (1), pp. 58-59, Jan 1996.

## Low-power spatial optical interconnection technique

*Continued from page 3.*

as high-resolution movie, for instance—but only need require small bits in response: such as **YES**, **1**, or **A**, etc.. Furthermore, since the location or direction of the My Button can be detected by the i-lidar indoor laser radar communication system *without* location information being explicitly sent, Button holders can automatically /receive various information services based on its location.

**Hideo Itoh, *Takeshi Akiyama, Takuichi Nishimura, Yoshinov Yamamoto, *Takehiko Hidaka, and Hideyuki Nakashima**
Cyber Assist Research Center,
AIST CREST, JST and
*Shonan Institute of Technology

**References**

1. http://www.vics.or.jp/eng/index.html
2. H. Nakashima and K. Hashida, *Location-based communication infrastructure for Situated Human Support*, **Proc. of World Multiconference on Systemics, Cybernetics and Informatics 2001** (SCI2001) IV, p47 2001.
3. H. Itoh, S. Yamamoto, M. Iwata, and Y. Yamamoto, *Guest guiding system based on the indoor laser radar system using HV targets and a frequency shifted feedback laser*, **Proc. of Int'l Topical Meeting on Contemporary Photonics Technologies 2000 (CPT2000), Tc-23**, pp.117-118 (2000).
4. http://www1.nsg.co.jp/umu/

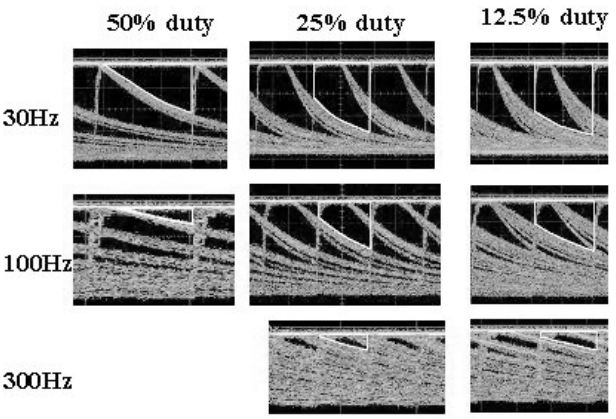


*Figure 3. Eye diagram of data transmission.*

# CALENDAR

## 2003

### SPIE's AeroSense

**Aerospace/Defense Sensing, Simulation, and Controls**
***21–25 April***
*Orlando, Florida USA*
Program • Advance Registration Ends 10 April 2003
Exhibition
URL: spie.org/conferences/Programs/03/or/

### Optical Data Storage

***11–14 May***
*Vancouver, BC Canada*
SPIE is a co-sponsor
Program
URL: www.osa.org/meetings/topicals/ODS/

**For More Information Contact**
**SPIE • PO Box 10, Bellingham, WA 98227-0010**
**Tel: +1 360 676 3290 • Fax: +1 360 647 1445 • E-mail: spie@spie.org • Web: www.spie.org**

### Microtechnologies for the New Millennium 2003

***19–21 May***
*Maspalomas, Gran Canaria, Canary Islands, Spain*
Program • Advance Registration Ends 9 May 2003
URL: spie.org/conferences/Programs/03/emt/

### Optics in Computing

***18–20 June***
*Washington, DC USA*
SPIE is a cooperating organization
Program
URL: www.osa.org/meetings/topicals/OC/

### The International Symposium on Optical Science and Technology

**SPIE's 48th Annual Meeting**
***3–8 August***
*San Diego, California USA*
Call for Papers • Abstracts Due 6 January 2003
Exhibition
URL: spie.org/conferences/calls/03/am/

### ITCom 2003

**Information Technologies and Communications**
***7–11 September***
*Orlando, Florida USA*
Co-located with NFOEC
Call for Papers • Abstracts Due 10 February 2003
URL: spie.org/conferences/calls/03/it/

### International Conference on Micro- and Nanoelectronics

***6–10 October***
*Zvenigorod, Russia*
Sponsored by SPIE Russia Chapter.
Program

## 2004

### Photonics West

***24–29 January***
*San Jose, California USA*
Program

# Join the Technical Group

## ...and receive this newsletter

### Membership Application

**Please Print** ☐ Prof. ☐ Dr. ☐ Mr. ☐ Miss ☐ Mrs. ☐ Ms.

First Name, Middle Initial, Last Name _____

Position _____ SPIE Member Number _____

Business Affiliation _____

Dept./Bldg./Mail Stop/etc. _____

Street Address or P.O. Box _____

City/State _____ Zip/Postal Code _____ Country _____

Telephone _____ Telefax _____

E-mail Address/Network _____

**Technical Group Membership fee is $30/year, or $15/year for full SPIE members.**

❑ Optics in Information Systems
**Total amount enclosed for Technical Group membership** **$** _____

❑ **Check enclosed.** Payment in U.S. dollars (by draft on a U.S. bank, or international money order) is required. Do not send currency. Transfers from banks must include a copy of the transfer order.

❑ **Charge to my:** ❑ VISA ❑ MasterCard ❑ American Express ❑ Diners Club ❑ Discover

Account # _____ Expiration date _____

Signature _____
*(required for credit card orders)*

This newsletter is printed as a benefit of the **Optics in Information Systems Technical Group.** Membership allows you to communicate and network with colleagues worldwide.

As well as a semi-annual copy of the *Optics in Information Systems* newsletter, benefits include SPIE's monthly publication, **oe***magazine*, and a membership directory.

SPIE members are invited to join for the reduced fee of $15. If you are not a member of SPIE, the annual membership fee of $30 will cover all technical group membership services. For complete information about SPIE membership and an application form, please contact us.

**Send this form (or photocopy) to:**
**SPIE • P.O. Box 10**
**Bellingham, WA 98227-0010 USA**
**Tel: +1 360 676 3290**
**Fax: +1 360 647 1445**
**E-mail: spie@spie.org**

**http://www.spie.org/info/ois**

**Please send me**
☐ Information about full SPIE membership
☐ Information about other SPIE technical groups
☐ FREE technical publications catalog

**Reference Code: 3537**

## OPTICSONLINE

### Optics Web Discussion Forum

You are invited to participate in SPIE's online discussion forum on Optics in Information Systems. To post a message, log in to create a user account. For options see "subscribe to this forum."

You'll find our forums well-designed and easy to use, with many helpful features such as automated email notifications, easy-to-follow 'threads,' and searchability. There is a full FAQ for more details on how to use the forums.

Main link to the new Optics in Information Systems forum:
`http://spie.org/app/forums/tech/`

Related questions or suggestions can be sent to `forums@spie.org`.

SPIE The International Society for Optical Engineering


# Optics in Information Systems

This newsletter is published semi-annually by SPIE—The International Society for Optical Engineering, for its International Technical Group on Optics in Information Systems.

*Editor and Technical Group Chairs* Bahram Javidi, Demetri Psaltis
*Technical Editor* Sunny Bains
*Managing Editor* Linda DeLano

Articles in this newsletter do not necessarily constitute endorsement or the opinions of the editors or SPIE. Advertising and copy are subject to acceptance by the editors.


SPIE is an international technical society dedicated to advancing engineering, scientific, and commercial applications of optical, photonic, imaging, electronic, and optoelectronic technologies. Its members are engineers, scientists, and users interested in the development and reduction to practice of these technologies. SPIE provides the means for communicating new developments and applications information to the engineering, scientific, and user communities through its publications, symposia, education programs, and online electronic information services.



**SPIE—The International Society for Optical Engineering,** P.O. Box 10, Bellingham, WA 98227-0010 USA. Tel: +1 360 676 3290. Fax: +1 360 647 1445.

**European Office:** Karin Burger, Manager, karin@spieeurope.org, Tel: +44 7974 214542. Fax: +44 29 2040 4873.

**In Japan:** c/o O.T.O. Research Corp., Takeuchi Bldg. 1-34-12 Takatanobaba, Shinjuku-ku, Tokyo 160, Japan. Tel: +81 3 3208 7821. Fax: +81 3 3200 2889. E-mail: otoresco@gol.com

**In Russia/FSU:** 12, Mokhovaja str., 121019, Moscow, Russia. Tel/Fax: +7 95 202 1079. E-mail: edmund@spierus.relcom.ru

# Planar integration of complex systems for optical communication and computing

The tremendous increase in performance of communication and computing hardware—which we have been observing for more than three decades—is based on a continued miniaturization and integration into monolithic blocks of ever more components and functionalities. In recent years, considerable effort has been made to transfer this concept to neighboring disciplines, in particular to mechanics and optics, to achieve a similar performance boost there. This will eventually lead to powerful complex micro-opto-electro-mechanical systems (MOEMS). However, integration approaches in these disciplines have to be sufficiently compatible with the (*de-facto*) standards set by microelectronics in order to be adopted and applied in commercial systems. For that reason, the concept of planar-integrated free-space optics[1] was developed.

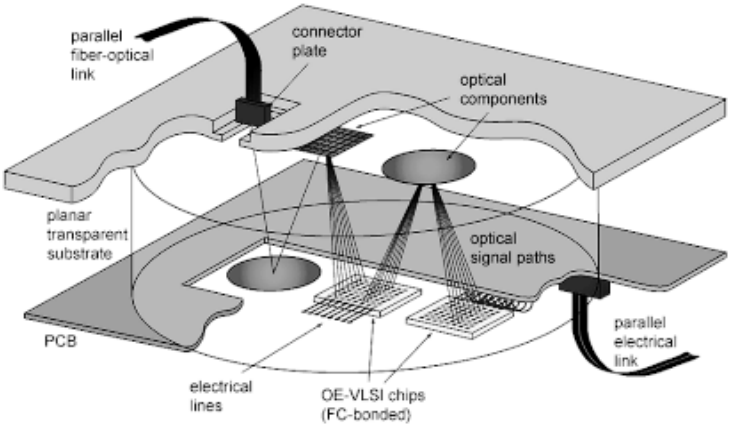


*Figure 1. Schematic of planar-integrated MOEMS with free-space optical interconnects.*

### *Planar integration of free-space optics*

This concept provides compatibility with microelectronics both in terms of dimensions and fabrication technologies. It thus makes the powerful parallel information processing tools of free-space optics available for VLSI. The idea is to miniaturize and "fold" a free-space optical setup into a transparent substrate of, typically, a few millimeter thickness in such a way that all optical components fall onto the plane-parallel surfaces. Passive components—like lenses or diffraction gratings—can then be realized through surface relief structuring, while active components (like optoelectronic chips with arrays of emitters, modulators, or detectors) can be bonded onto the substrate. A reflective coating ensures that optical signals propagate along zigzag paths inside the substrate (see Figure 1).

Since all passive components are located at the substrate surfaces, the optical system can be fabricated as a whole using mask-based techniques. This approach provides lithographic precision concerning the positioning of components, and high accuracy for the required relief structures because the well-established and sophisticated etching techniques of the semiconductor industry can be applied. Due to the integration into a rigid substrate, the passive optical system does not require further adjustment and it is well-protected against deleterious environmental influences.

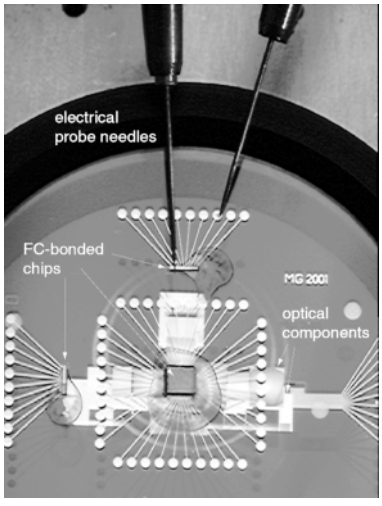


*Figure 2. Experimental demonstrator implementing an optical crossbar switch.*

From a topological point of view, the planar-integration approach yields a fully three-dimensional (3D) system architecture but requires only two-dimensional (2D) fabrication complexity. This allows one to implement highly-parallel and complex (regular and irregular) optical interconnect schemes involving large fan-out, fan-in, and filtering operations that would be difficult to implement otherwise. Experimental demonstrations include point-to-point interconnection of 2500 channels in a multi-chip module architecture,[2] optical 1-to-10 fan-out and 10-to-1 fan-in in an integrated 10×10 crossbar architecture,[3] and optical correlation.[4] In all three cases, the channel density is typically 400mm$^{-2}$. Thus, crucial requirements for interconnects—such as those envisaged by the ITRS roadmaps for the near future—can be met.

### *Planar-integrated MOEMS*

In addition to housing the free-space optical system, the transparent substrate can also serve as a board for electrical circuitry as indicated in Figure 1. In an experimental demonstration, electrical wires and bond pads were realized through lithographic structuring and evaporation of metals (aluminum, gold). Optoelectronic chips were then flip-chip bonded onto the transparent substrate. Figure 2 shows an optoelectronic MOEMS fabricated in this way. It comprises three chips and implements a 10×10 crossbar switch.[3] Optical signals are generated by two linear arrays of VCSEL diodes and

*Continues on page 8.*

SPIE Society of Photo-Optical Instrumentation Engineers

P.O. Box 10 • Bellingham, WA 98227-0010 USA

Change Service Requested

**DATED MATERIAL**

Non-Profit Org.
U.S. Postage Paid
Society of
Photo-Optical
Instrumentation
Engineers